

# Molecular structures of tetraborane(10) derivatives: *ab initio* calculations for $H_2MB_3H_8$ (M = B, Al, Ga or In) and gas-phase electron diffraction study of $H_2GaB_3H_8$ †

Carole A. Morrison,<sup>a</sup> Bruce A. Smart,<sup>a</sup> Paul T. Brain,<sup>a</sup> Colin R. Pulham,<sup>a</sup> David W. H. Rankin <sup>\*,a</sup> and Anthony J. Downs<sup>b</sup>

<sup>a</sup> Department of Chemistry, University of Edinburgh, West Mains Road, Edinburgh, UK EH9 3JJ

<sup>b</sup> Inorganic Chemistry Laboratory, University of Oxford, South Parks Road, Oxford, UK OX1 3QR

Structural trends in the family of compounds  $H_2MB_3H_8$  (M = B, Al, Ga or In) have been investigated by *ab initio* molecular orbital calculations. In addition, the molecular structure of the *arachno* borane  $H_2GaB_3H_8$  has been re-determined by gas-phase electron diffraction using the SARACEN method of structural analysis. Salient structural parameters ( $r_e$ ) were found to be:  $r[B(1)\cdots Ga(2)]$  231.0(2),  $r[B(1)-B(3)]$  177.9(13),  $r[B(1)-B(4)]$  184.0(13),  $r[B(1)-H(1,2)]$  123.0(11),  $r[Ga(2)-H(1,2)]$  181(4),  $r[B(1)-H(1,4)]$  123.7(11),  $r[B(4)-H(1,4)]$  142.2(18) pm; butterfly angle 117.1(7)°.

Using gas-phase electron diffraction (GED) data alone, it is often not possible to obtain a complete structural determination of a molecule.<sup>1</sup> This is both because light atoms (normally hydrogen) are poor scatterers of electrons and also because similar interatomic distances lead to strong correlation effects between refining parameters. To overcome this limitation, GED data can be supplemented with data from other sources; traditionally this has involved other experimental techniques, such as microwave (MW) or liquid-crystal NMR (LCNMR) spectroscopy.<sup>1</sup> The structural group at Edinburgh has recently developed a new method called SARACEN (Structure Analysis Restrained by *Ab initio* Calculations for Electron diffractionN)<sup>2,3</sup> aimed at exploiting the rapid developments in the field of computational chemistry, where recent improvements in both computer technology and software have allowed increasingly more sophisticated calculations to be run routinely. The SARACEN method supplements the electron-diffraction data with predicate observations<sup>4</sup> in the form of restraints derived from a series of *ab initio* calculations. Potentially, all parameters needed to define the molecular structure may then be refined, yielding a structure of greater reliability, and with more realistic estimated errors, than that derived from the GED data alone.

Many of the smaller boron hydrides, *e.g.*  $B_4H_{10}$  and its derivatives, are volatile liquids under ambient conditions and if the structures of the gaseous molecules are to be deduced GED will often be the only viable method. Moreover, as all these molecules have several similar B–B and B–H distances, the SARACEN method will be required in order to obtain the most reliable structures from the available data.

A study of a series of structurally related compounds may be expected to reveal trends that are often related to changes in physical properties, reactivity, *etc.* The series of compounds under investigation here involves the substitution of one wing boron atom in tetraborane(10) with another Group 13 element, *viz.* aluminium, gallium or indium. The four structures have

all been investigated using *ab initio* computations, and, for  $H_2GaB_3H_8$ , by gas-phase electron diffraction. A structure for this compound had already been reported,<sup>5</sup> but the development of the SARACEN method has enabled an improved structure now to be deduced from the original data. In addition, the development of reliable *ab initio* harmonic force fields has allowed the calculation of the vibrational corrections needed in the GED refinement, information which was not available at the time of the original refinement. For these reasons, a new refinement is now reported. The results from the *ab initio* calculations on molecules in the series  $H_2MB_3H_8$  (M = B, Al, Ga or In) are presented first, followed by the SARACEN refinement of the GED data for  $H_2GaB_3H_8$ . The structural trends identified within the series by the calculations are then discussed. This paper represents the first part of a project relating to Group 13 derivatives of  $B_4H_{10}$ . Results for the series  $(CH_3)_2MB_3H_8$  (M = B, Al, Ga or In) will be presented subsequently.<sup>6</sup>

## Experimental

### (a) *Ab initio* calculations

**Theoretical methods.** All calculations were carried out on a DEC Alpha APX 1000 workstation using the GAUSSIAN suite of programs.<sup>7</sup>

**Geometry optimisations.** A graded series of calculations was performed for each of the four compounds in order to gauge the effects of basis set and electron correlation treatments on the optimised structures. Calculations were performed using standard gradient techniques at the SCF level of theory using the 6-31G<sup>\*8-10</sup> and 6-311G<sup>\*\*11,12</sup> basis sets. In the case of indium, where no standard 6-31G<sup>\*</sup> or 6-311G<sup>\*\*</sup> basis set is available, a basis set due to Huzinaga<sup>13</sup> was used with an additional diffuse d-polarisation function (exponent 0.10), contracted to (21s, 17p, 11+1d)/[15s, 12p, 7+1d]. This was deployed to describe indium throughout the higher calculations performed. We also wished to investigate the effects of diffuse functions on heavy (*i.e.* non-hydrogen) atoms and accordingly the 6-31 + G<sup>\*</sup> basis set was employed in the  $B_4H_{10}$  and  $H_2AlB_3H_8$  calculations.

The GAUSSIAN frozen-core (FC) approximation divides electrons into two categories, core and valence, with only the valence electrons considered in the electron-correlation treat-

† Supplementary data available: tables of *ab initio* geometries and energies for all calculations, and Cartesian coordinates from the 6-311G<sup>\*\*</sup>/MP2 *ab initio* calculation for  $H_2MB_3H_8$  (M = B, Al, Ga or In), and final coordinates and least-squares correlation matrix for the SARACEN study of  $H_2GaB_3H_8$ . For direct electronic access see <http://www.rsc.org/suppdata/dt/1998/2147/>, otherwise available from BLDSC (No. SUP 57390, 12 pp.) or the RSC Library. See Instructions for Authors, 1998, Issue 1 (<http://www.rsc.org/dalton>).

**Table 1** GED data analysis parameters for H<sub>2</sub>GaB<sub>3</sub>H<sub>8</sub>

Camera distance/ mm	Weighting functions/nm <sup>-1</sup>					Correlation parameter	Scale factor, <i>k</i> <sup>a</sup>	Electron wavelength <sup>b</sup> /pm
	$\Delta s$	$s_{\min}$	$sw_1$	$sw_2$	$s_{\max}$			
201.08	4	52	72	176	208	0.3799	0.584(30)	5.670
259.48	2	20	40	140	160	0.1114	0.760(29)	5.671

<sup>a</sup> Figures in parentheses are the estimated standard deviations. <sup>b</sup> Determined by reference to the scattering patterns of benzene vapour.

ment. The default GAUSSIAN FC approximation satisfactorily classified the electrons of boron and aluminium as core or valence but unsatisfactorily placed the gallium 3d<sup>10</sup> (and indium 4d<sup>10</sup>) electrons in the core region, whereas a close consideration of orbital energies clearly showed that these outer core orbitals lay closer in energy to the 4s and 4p (or 5s and 5p) valence orbitals than to the remaining inner core orbitals. Calculations were therefore performed with the d orbitals of gallium and indium considered as valence rather than core functions, thereby including an additional ten electrons in the electron-correlation treatment, which was performed at MP2 level for H<sub>2</sub>GaB<sub>3</sub>H<sub>8</sub> and H<sub>2</sub>InB<sub>3</sub>H<sub>8</sub>. The default FC approximation was used for the elements boron and aluminium in B<sub>4</sub>H<sub>10</sub> and H<sub>2</sub>AlB<sub>3</sub>H<sub>8</sub> in calculations to the levels MP2, MP3, MP4SDQ and QCISD, all with the 6-31G\* basis set.

**Frequency calculations.** Frequency calculations were performed at the 6-31G\*/MP2 level for tetraborane(10), confirming C<sub>2v</sub> as a local minimum on the potential-energy surface. For the remaining compounds, frequency calculations were performed at the 6-31G\*/SCF level, confirming C<sub>s</sub> symmetry in all three cases. For H<sub>2</sub>GaB<sub>3</sub>H<sub>8</sub> the force field described by Cartesian force constants at the 6-31G\*/SCF level was transformed into one described by a set of symmetry coordinates using the program ASYM40.<sup>14</sup> As no complete assignment of the infrared and Raman spectra is available, it was not possible to scale the *ab initio* force constants using experimental frequencies. Instead, as the best alternative, the force constants were scaled empirically using scaling factors of the order of 0.94 for bond stretches, 0.96 for angle bending and 0.92 for torsions.<sup>‡</sup>

### (b) Gas-phase electron diffraction (GED)

**GED data.** The new refinement for H<sub>2</sub>GaB<sub>3</sub>H<sub>8</sub> reported here is based on the original data set,<sup>5</sup> recorded on the Edinburgh apparatus. It should be noted that the H<sub>2</sub>GaB<sub>3</sub>H<sub>8</sub> vapour was found to react with the emulsion of the photographic plates, resulting in higher than normal noise levels in the GED data sets. Standard programs were used for the data reduction<sup>15</sup> with the scattering factors of Ross *et al.*<sup>16</sup> The weighting points used in setting up the off-diagonal weight matrix, the *s* range, scale factors, correlation parameters and electron wavelengths are given in Table 1.

**GED model.** The molecular framework and atom numbering scheme of H<sub>2</sub>GaB<sub>3</sub>H<sub>8</sub> are shown in Fig. 1. As the SARACEN method removes the need to make any structural assumptions, the new model written for this re-refinement includes six more geometric parameters than the original.<sup>5</sup> The six extra parameters allow for the deviation of the bridging hydrogen atoms from the heavy atom planes Ga(2)–B(1)–B(3) and B(1)–B(4)–B(3), tilting of the terminal BH<sub>2</sub> and GaH<sub>2</sub> units in or out of the heavy atom cage and, finally, differences between the terminal distances *r*B(4)–H(4)<sub>endo</sub> and *r*B(4)–H(4)<sub>exo</sub> [and *r*Ga(2)–H(2)<sub>endo</sub> and *r*Ga(2)–H(2)<sub>exo</sub>]. These three structural features were found to be significant in the recent structural re-refinement of the parent compound B<sub>4</sub>H<sub>10</sub>.<sup>3</sup> Moreover, in

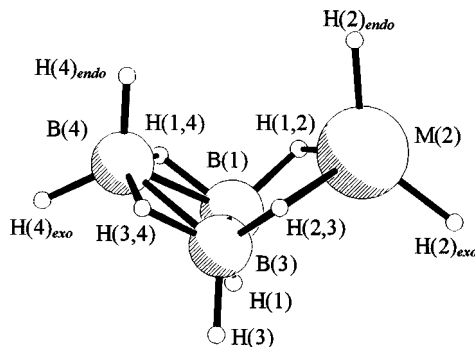


**Fig. 1** Molecular framework of H<sub>2</sub>MB<sub>3</sub>H<sub>8</sub> [M = B, Al, Ga or In]

an effort to reduce correlation effects several of the original parameters describing similar bond distances have been re-defined as weighting averages and differences, rather than defined separately.

A total of twenty geometric parameters are therefore used to define the structure in C<sub>s</sub> symmetry in this new refinement, as documented in Table 2. The gallium and boron cage atoms require four parameters to define their positions, *viz.* a weighted average and difference of the two B–B distances (*p*<sub>1</sub> and *p*<sub>2</sub>), *r*(B...Ga) (*p*<sub>3</sub>) and the butterfly angle (*p*<sub>18</sub>), defined as the angle between the planes B(1)–B(4)–B(3) and B(1)–Ga(2)–B(3). The other nine distance parameters, five bond angle parameters and two torsion angles locate the positions of the ten hydrogen atoms in the structure. Parameter *p*<sub>4</sub> is defined as *r*[Ga(2)–H(1,2)], *p*<sub>5</sub> as the weighted average of the B–H distances and *p*<sub>6</sub> as the average B–H bridge distance minus the average B–H terminal distance. Parameter *p*<sub>7</sub> is the difference between the outer B(4)–H(1,4) bridging distance and the average of the two inner bridging distances {*r*[B(1)–H(1,2)] and *r*[B(1)–H(1,4)]}, *p*<sub>8</sub> is *r*[B(1)–H(1,4)] minus *r*[B(1)–H(1,2)], *p*<sub>9</sub> is the difference between the terminal distances *r*B(1)–H(1) and the average B–H<sub>endo/exo</sub> distance, and *p*<sub>10</sub> is [*r*[B–H(4)<sub>endo</sub>] minus *r*[B–H(4)<sub>exo</sub>]]. Parameters *p*<sub>11</sub> and *p*<sub>12</sub> are defined as the average and difference of the two terminal Ga–H distances. The five bond angle parameters required are B(3)–B(1)–H(1) (*p*<sub>13</sub>), H(2)<sub>endo</sub>–Ga(2)–H(2)<sub>exo</sub> (*p*<sub>14</sub>), H(4)<sub>endo</sub>–B(4)–H(4)<sub>exo</sub> (*p*<sub>15</sub>), and the GaH<sub>2</sub> and BH<sub>2</sub> wing tilt angles (*p*<sub>16</sub> and *p*<sub>17</sub>) defined as the angles between the bisectors of the H(2)<sub>endo</sub>–Ga(2)–H(2)<sub>exo</sub> and H(4)<sub>endo</sub>–B(4)–H(4)<sub>exo</sub> wing angles and the planes B(1)–Ga(2)–B(3) and B(1)–B(4)–B(3), respectively, a positive value indicating a tilt into the cage structure. The remaining two torsional angles are defined as ‘H(1,2) dip’ (*p*<sub>19</sub>) describing the elevation of the bridging atom H(1,2) above the B(1)–Ga(2)–B(3) plane [*i.e.* the angle between the planes B(1)–Ga(2)–B(3) and B(1)–Ga(2)–H(1,2)] and ‘H(1,4) dip’ (*p*<sub>20</sub>) describing similarly the elevation of the H(1,4) bridging atom above the B(1)–B(4)–B(3) plane.

## Results and Discussion

### (a) *Ab initio* calculations

Some geometry optimisations for B<sub>4</sub>H<sub>10</sub> have been reported previously, being performed at the 3-21G\*/SCF, 6-31G\*/SCF, 6-31G\*/MP2 and 6-31G\*\*/MP2 levels.<sup>17</sup> This range was

<sup>‡</sup> Scale factors used as for B<sub>4</sub>H<sub>10</sub>.<sup>3</sup>

**Table 2** Geometrical parameters<sup>a,b</sup> for the SARACEN<sup>c</sup> study of H<sub>2</sub>GaB<sub>3</sub>H<sub>8</sub> (*r*<sub>a</sub><sup>o</sup>/pm, angles<sub>a</sub> in °)

Parameter Independent	Results <sup>d</sup>	
<i>p</i> <sub>1</sub>	av. <i>r</i> (B–B)	182.0(12)
<i>p</i> <sub>2</sub>	diff. <i>r</i> (B–B)	6.0(10)
<i>p</i> <sub>3</sub>	<i>r</i> [B(1)···Ga(2)]	231.0(2)
<i>p</i> <sub>4</sub>	<i>r</i> [Ga(2)–H(1,2)]	181(4)
<i>p</i> <sub>5</sub>	av. <i>r</i> (B–H)	124.5(5)
<i>p</i> <sub>6</sub>	av. <i>r</i> (B–H <sub>b</sub> ) – av. <i>r</i> (B–H <sub>t</sub> )	12.8(14)
<i>p</i> <sub>7</sub>	diff. [ <i>r</i> (B–H <sub>b</sub> )] (outer – inner)	18.9(22)
<i>p</i> <sub>8</sub>	diff. [ <i>r</i> (B–H <sub>b</sub> )] (inner)	0.8(10)
<i>p</i> <sub>9</sub>	<i>r</i> [B(1)–H(1)] – av. <i>r</i> [B(4)–H <sub>i</sub> ]	–0.7(3)
<i>p</i> <sub>10</sub>	diff. <i>r</i> (B–H <sub>i</sub> ) ( <i>endo</i> – <i>exo</i> )	0.3(1)
<i>p</i> <sub>11</sub>	av. <i>r</i> (Ga–H <sub>t</sub> )	149.3(14)
<i>p</i> <sub>12</sub>	diff. <i>r</i> (Ga–H <sub>t</sub> ) ( <i>endo</i> – <i>exo</i> )	0.2(1)
<i>p</i> <sub>13</sub>	B(3)–B(1)–H(1)	111.6(10)
<i>p</i> <sub>14</sub>	H(2) <sub>endo</sub> –Ga(2)–H(2) <sub>exo</sub>	131.0(19)
<i>p</i> <sub>15</sub>	H(4) <sub>endo</sub> –B(4)–H(4) <sub>exo</sub>	119.2(10)
<i>p</i> <sub>16</sub>	GaH <sub>2</sub> tilt	–2.5(6)
<i>p</i> <sub>17</sub>	BH <sub>2</sub> tilt	0.7(7)
<i>p</i> <sub>18</sub>	Butterfly angle	117.1(7)
<i>p</i> <sub>19</sub>	H(1,2) dip	10.7(10)
<i>p</i> <sub>20</sub>	H(1,4) dip	0.3(2)
Dependent		
	B(1)–B(4)–B(3)	57.8(3)
	B(1)–Ga(2)–B(3)	45.3(4)
	<i>r</i> [B(1)–B(3)]	177.9(13)
	<i>r</i> [B(1)–B(4)]	184.0(13)
	<i>r</i> [B(1)–H(1,4)]	123.7(11)
	<i>r</i> [B(4)–H(1,4)]	142.2(18)
	<i>r</i> [B(1)–H(1,2)]	123.0(11)
	<i>r</i> [B(1)–H(1)]	116.6(8)
	<i>r</i> [B(4)–H(4) <sub>endo</sub> ]	117.1(8)
	<i>r</i> [B(4)–H(4) <sub>exo</sub> ]	116.8(8)
	<i>r</i> [Ga(2)–H(2) <sub>endo</sub> ]	149.4(14)
	<i>r</i> [Ga(2)–H(2) <sub>exo</sub> ]	149.2(14)

<sup>a</sup> For definition of parameters see the text; b = bridging, t = terminal. <sup>b</sup> For atom numbering see Fig. 1. <sup>c</sup> For details of refinement see the text and Table 5. <sup>d</sup> Estimated standard deviations (e.s.d.s), derived from the least-squares refinement are given in parentheses.

recently extended<sup>3</sup> to include two larger basis sets (6-31+G\*, to assess the effects of diffuse functions on the B atoms, and a TZP basis set composed of Dunning's TZ basis set<sup>18</sup> augmented with one set of d-polarisation functions on B and one set of p-polarisation functions on H) and two higher levels of theory [MP3 and CCSD(T)]. To allow a direct comparison with calculations performed for H<sub>2</sub>AlB<sub>3</sub>H<sub>8</sub> (see below), this range has now been extended further to include the 6-311G\*\* basis set at the SCF and MP2 levels, and the 6-31G\* basis set as MP4 and QCISD levels of electron correlation treatment. Some calculations for H<sub>2</sub>GaB<sub>3</sub>H<sub>8</sub> have also been reported, at 3-21G\*/SCF,<sup>19</sup> DZ/SCF<sup>20</sup> and single-point calculations at the 3-21G\*/MP4 level.<sup>19</sup> This range of calculations is now extended to include the effects of further improvements in basis set to 6-311G\*\* and electron correlation at the MP2 level.

In light of the many calculations performed on this series of compounds the results obtained are confined to SUP 57390 Tables 1–4. Results obtained from the highest level calculations, 6-311G\*\*/MP2, are reported for all four compounds in Table 3 of this paper.

Several changes in geometry observed with improvements in calculation level (some of which have been discussed previously for B<sub>4</sub>H<sub>10</sub><sup>3</sup>) were found for all four compounds of the series, and are reported below. In general, it was observed that the most significant changes in geometry occurred with the introduction of electron correlation at the MP2 level, with smaller changes arising from improvements in basis set.

**Cage structure.** The cage distance *r*[B(1)–B(3)] for all four

**Table 3** Structural trends observed in the H<sub>2</sub>MB<sub>3</sub>H<sub>8</sub> series (M = B, Al, Ga or In) by *ab initio* (6-311G\*\*/MP2)<sup>a</sup> calculations (*r*<sub>a</sub>/pm, angles in °)

Fragment	Parameter <sup>b</sup>	M			
		B	Al	Ga	In
Fragment	Covalent radius <sup>c</sup>	88	125	125	140
	Ionic radius <sup>c</sup>	—	68	76	94
	Mulliken charge <sup>d</sup>	–0.2	+0.8	+0.5	+0.7
Cage	<i>r</i> [B(1)–B(3)]	173.1	178.1	178.4	179.6
	<i>r</i> [B(1)–B(4)]	185.6	185.0	184.6	183.9
	<i>r</i> [B(1)···M(2)]	185.6	228.0	229.1	253.1
	Butterfly angle	116.6	116.0	116.7	117.9
Bridge	<i>r</i> [B(1)–H(1,2)]	125.6	124.3	125.0	124.8
	<i>r</i> [M(2)–H(1,2)]	142.0	181.3	182.8	203.2
	<i>r</i> [B(1)–H(1,4)]	125.6	125.6	125.6	125.7
	<i>r</i> [B(4)–H(1,4)]	142.0	141.5	141.8	142.1
	B(1)–H(1,2)–M(2)	87.6	94.7	94.4	97.1
	H(1,2) dip	8.4	10.6	10.5	12.9
Terminal	H(1,4) dip	8.4	2.4	0.3	3.0
	<i>r</i> [M(2)–H(2) <sub>endo</sub> ]	119.5	156.6	153.5	172.5
	<i>r</i> [M(2)–H(2) <sub>exo</sub> ]	118.9	156.5	153.3	172.4
	<i>r</i> [B(4)–H(4) <sub>endo</sub> ]	119.5	119.4	119.5	119.6
	<i>r</i> [B(4)–H(4) <sub>exo</sub> ]	118.9	119.2	119.2	119.3
	<i>r</i> [B(1)–H(1)]	118.2	118.6	118.6	118.8
	H(2) <sub>endo</sub> –M(2)–H(2) <sub>exo</sub>	119.7	128.2	131.4	134.1
H(4) <sub>endo</sub> –B(4)–H(4) <sub>exo</sub>	119.7	119.0	119.0	118.7	
B(3)–B(1)–H(1)	114.7	112.1	111.8	111.2	

<sup>a</sup> For In basis set see the text. <sup>b</sup> For definition of parameters see the text. <sup>c</sup> Ref. 21. <sup>d</sup> Taken from *ab initio* 6-311G\*\*/MP2 calculations.

compounds was found to be equally sensitive to improvements in basis set quality on going from 6-31G\* to 6-311G\*\*, lengthening by *ca.* 0.3 pm at SCF and *ca.* 1 pm at the MP2 level. The distance *r*[B(1)–B(4)] was also found to behave similarly in all compounds (except H<sub>2</sub>GaB<sub>3</sub>H<sub>8</sub>), increasing by less than 1 pm at SCF and by about 1.5 pm at the MP2 level of theory for improvements in basis set treatment. In H<sub>2</sub>GaB<sub>3</sub>H<sub>8</sub> the distance shortens by 3.5 pm at the SCF level and remains largely unchanged at the MP2 level of theory. The introduction of electron correlation at the MP2 level showed marked similarities for all four compounds, with *r*[B(1)–B(3)] shortening by about 2 pm and *r*[B(1)–B(4)] shortening by 3–7 pm with both 6-31G\* and 6-311G\* basis sets. Higher levels of theory (MP3, MP4 and QCISD) employed in calculations for B<sub>4</sub>H<sub>10</sub> and H<sub>2</sub>AlB<sub>3</sub>H<sub>8</sub> have no further significant effect on *r*[B(1)–B(3)], and slightly lengthen *r*[B(1)–B(4)]. It is worth noting that in calculations performed for all four compounds *r*[B(1)–B(4)] changes more than *r*[B(1)–B(3)] with improvements in both basis set and level of theory.

Of particular interest is the very marked variation in the bond distance B···M (M = Al, Ga or In) with improving basis set and level of theory. Changing the basis set from 6-31G\* to 6-311G\*\* results in *r*(B···M) lengthening [except *r*(B···Al) and *r*(B···In) which shorten at the SCF level by 0.5 and 1.6 pm, respectively]. The effect is particularly dramatic for H<sub>2</sub>GaB<sub>3</sub>H<sub>8</sub>, for which *r*(B···Ga) was found to lengthen by 4.6 pm at the MP2 level (7.9 pm SCF) with the basis set improvement. This considerable change can be partly attributed to the poor quality of the Ga 6-31G\* basis set, which includes an insufficient number of basis functions describing the core region of such a large atom. Electron correlation to the MP2 level was found to shorten *r*(B···M) in all three molecules; by about 3 pm using both the 6-31G\* and 6-311G\*\* basis sets for H<sub>2</sub>AlB<sub>3</sub>H<sub>8</sub>, 3 pm with the 6-31G\* basis set (6 pm with 6-311G\*\*) for H<sub>2</sub>GaB<sub>3</sub>H<sub>8</sub>, and an average of 8.5 pm for H<sub>2</sub>InB<sub>3</sub>H<sub>8</sub> with both basis sets.

**Bridge region.** The bridging B–H distances were in general found to be less sensitive to change than the B–B/M cage

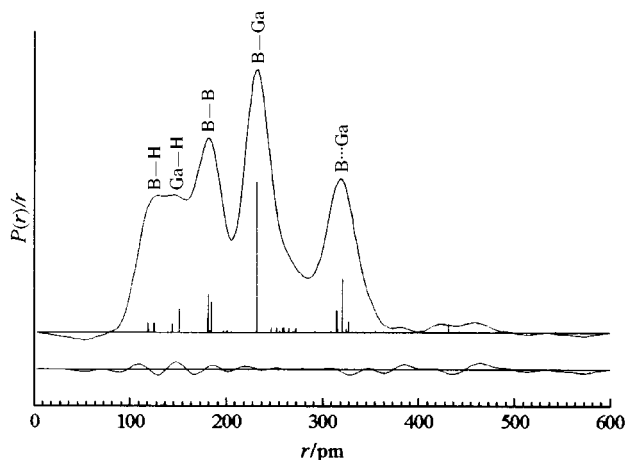


Fig. 2 Observed and final difference radial-distribution curves for  $\text{H}_2\text{GaB}_3\text{H}_8$ . Before Fourier inversion the data were multiplied by  $s \cdot \exp[(-0.000\ 02s^2)(Z_{\text{Ga}} - f_{\text{Ga}})(Z_{\text{B}} - f_{\text{B}})]$

distances for all four compounds. Variations were generally observed to be about 1 pm on improving the basis set from 6-31G\* to 6-311G\*\* at both the SCF and MP2 levels of theory, with the exception of  $r[\text{B}(4)\text{--H}(1,4)]$  in  $\text{H}_2\text{GaB}_3\text{H}_8$  which lengthened by *ca.* 5 pm at the SCF and *ca.* 3 pm at the MP2 levels of theory. Similarly, introducing electron correlation to the MP2 level resulted in changes averaging about 1 pm, with the exception of  $r[\text{B}(4)\text{--H}(1,4)]$  in  $\text{H}_2\text{InB}_3\text{H}_8$  which shortened by about 2.5 pm using both basis sets.

The M–H bridging distances (where M = B, Al or In) were largely unaffected by improvements in basis set and level of theory, with changes averaging about 1 pm. The exception was  $r[\text{Ga}(2)\text{--H}(1,2)]$  which was found to be heavily dependent on improvements in basis set as a result of the poor quality of 6-31G\*, shortening by *ca.* 4 pm at the SCF and *ca.* 6 pm at the MP2 level of theory for improving the basis set to 6-311G\*\*.

**Terminal region.** For all four compounds the B–H terminal bond distances were found to be largely insensitive to basis set quality and level of theory. For the terminal M–H distances improvements in basis set quality at the SCF level result in only minor changes (generally less than 0.2 pm); at the MP2 level the distances shorten by *ca.* 1, 3 or 2 pm, where M = Al, Ga or In, respectively. Electron correlation predicts all  $\text{M}(2)\text{--H}(2)_{\text{endolexo}}$  distances to vary by less than 1 pm, with the exceptions of the Ga and In distances which shorten by 2 pm with the 6-311G\*\* basis set.

#### (b) Gas-phase electron diffraction study of $\text{H}_2\text{GaB}_3\text{H}_8$

As already mentioned, the new structure presented here is a re-refinement of the original GED data.<sup>5</sup> Many assumptions had to be made in the first attempt as it was found that the refinement was much hampered by the marked correlation between several parameters, with *e.g.* B–B and Ga–H<sub>b</sub> distances lying close together on the radial-distribution curve (see Fig. 2). Moreover, the problems encountered were exacerbated by the degree to which the molecular scattering is dominated by the heavier atoms, making it particularly difficult to locate precisely the positions of the hydrogen atoms. Accordingly the following assumptions had to be made in the original refinement: (i) some of the parameters defining the structure of the  $\text{B}_3\text{H}_8$  group were fixed at corresponding values determined in the original  $\text{B}_4\text{H}_{10}$  study;<sup>22</sup> (ii) the differences between the three different B–H<sub>b</sub> distances were set at zero; (iii) the bridging hydrogen atoms were taken to lie in the heavy-atom planes Ga(2)–B(1)–B(3) and B(1)–B(4)–B(3); (iv) the angle  $\text{H}(2)_{\text{endo}}\text{--Ga}(2)\text{--H}(2)_{\text{exo}}$  was fixed at 115°; and (v) as no force field was available, vibrational amplitudes were assigned values based on studies of similar

compounds carried out at that time, *e.g.*  $\text{B}_4\text{H}_{10}$ ,<sup>22</sup>  $\text{Me}_2\text{GaB}_3\text{H}_8$ <sup>23</sup> and  $[\text{H}_2\text{GaCl}]_2$ .<sup>24</sup> In total, six geometric parameters and five amplitudes of vibration could be refined in the first structural analysis.<sup>5</sup> Several of the features deduced in this refinement were, however, contrary to the findings on similar structures made by other methods. In particular, the Ga–H<sub>t</sub> distance was found to be one of the shortest measured for a gallium hydride, although the vibrational spectrum gave every reason to expect the distance to be comparable with those in other compounds.<sup>5</sup> Moreover, the subsequent *ab initio* calculations showed  $r(\text{Ga}\text{--H}_b)$  to be significantly longer than measured, the three B–H<sub>b</sub> distances quite distinct and  $\text{H}(2)_{\text{endo}}\text{--Ga}(2)\text{--H}(2)_{\text{exo}}$  significantly wider than 115°.

Results afforded by the new refinement of the structure of  $\text{H}_2\text{GaB}_3\text{H}_8$  are given in Table 2. Of the twenty geometric parameters only three refined well without the inclusion of restraints, *viz.*  $r(\text{B}\text{--B})$  ( $p_1$ ),  $r(\text{B}\cdots\text{Ga})$  ( $p_3$ ) and the butterfly torsional angle ( $p_{18}$ ). Parameters  $p_5$  [*av.*  $r(\text{B}\text{--H})$ ] and  $p_{11}$  [*av.*  $r(\text{Ga}\text{--H})$ ], which correspond to distances located on the first peak of the radial-distribution curve, refined to values somewhat shorter than expected, compared with the results obtained for the parent  $\text{B}_4\text{H}_{10}$  compound<sup>3</sup> and the structure calculated *ab initio*. The average B–H distance had refined unrestrained to 122.4(6) pm, about 3 pm shorter than expected, and the average Ga–H terminal distance to 147.2(12) pm, 6 pm less than calculated *ab initio*. In view of these significant differences, it was decided that both parameters should be restrained in accordance with the SARACEN method, with restraints constructed as shown in Table 4(a).§ The refined parameters are then the best to fit all available information, both experimental and theoretical, and represent the most probable structure, avoiding subjective preference for one particular type of data.

The remaining fifteen geometric parameters, which describe the location of the hydrogen atoms, required restraints in order to complete the structural refinement.¶ This was expected since the heavy gallium atom and, to a lesser extent the boron atoms, dominate the molecular scattering. It is clearly demonstrated on the radial distribution curve (Fig. 2) that the distance  $\text{B}(1)\cdots\text{Ga}(2)$ , at 231.0 pm, is by far the most prominent feature. Other structural information is somewhat suppressed and locating the hydrogen atoms is particularly difficult as a result.

In addition to geometric restraints, the SARACEN method allows restraints to be applied to ratios of amplitudes of vibration corresponding to electronically similar pairs of atoms separated by similar distances or, if necessary, directly to amplitudes that could not otherwise be refined independently. Values for amplitude restraints are calculated directly from the scaled force field, with uncertainty ranges of 5% considered appropriate for amplitude ratios or 10% for absolute values. For  $\text{H}_2\text{GaB}_3\text{H}_8$  only two out of the fifty-five amplitudes of vibration could be refined freely, *viz.*  $\text{B}(1)\cdots\text{Ga}(2)$  ( $u_{12}$ ) and  $\text{B}(4)\cdots\text{Ga}(2)$  ( $u_{15}$ ). By the inclusion of the five amplitude

§ Each geometric restraint has a value and an uncertainty derived from the graded series of *ab initio* calculations. Absolute values are taken from the highest level calculation and uncertainties are estimated from values given by lower level calculations, or based on a working knowledge of the reliability of the calculations for electronically similar molecules.

¶ As a result of the large number of basis functions required to describe  $\text{H}_2\text{GaB}_3\text{H}_8$  it was not possible to perform calculations to a high enough level to display satisfactory convergence (see SUP 57390 Table 3). However, the large array of calculations performed on the parent compound  $\text{B}_4\text{H}_{10}$  (SUP 57390 Table 1) shows that the heavy cage atoms are much better described at the MP2 level of electron correlation than at the SCF level. For this reason the uncertainty of 1 pm chosen for the cage parameter diff.  $r(\text{B}\text{--B})$  ( $p_2$ ) is based on the variation observed in the B–B cage distances of  $\text{B}_4\text{H}_{10}$  for calculations performed at MP2 level and above. The derivation of the remaining geometric restraints is based on results obtained from the  $\text{H}_2\text{GaB}_3\text{H}_8$  series of calculations, and is documented in Table 4(a).

**Table 4** Derivation of the restraints used in the SARACEN study of  $\text{H}_2\text{GaB}_3\text{H}_8$  ( $r_e/\text{pm}$ , angles in  $^\circ$ )

(a) Geometric restraints		6-31G*/SCF	6-311G**/SCF	6-31G*/MP2 <sup>b</sup>	6-311G**/MP2 <sup>b</sup>	Values used
$p_2$	diff. $r(\text{B}-\text{B})$	12.2	8.3	7.0	6.2	6.2(10)
$p_4$	$r[\text{Ga}(2)-\text{H}(1,2)]$	188.2	184.1	188.4	182.8	183(6)
$p_5$	av. $r(\text{B}-\text{H})$	125.1	126.2	125.5	126.1	126.1(6)
$p_6$	av. $r(\text{B}-\text{H}_b) - \text{av. } r(\text{B}-\text{H}_i)$	10.8	12.7	10.4	11.7	11.7(13)
$p_7$	av. $r(\text{B}-\text{H}_b)$ (outer - inner)	13.6	17.9	14.0	16.5	16.5(25)
$p_8$	diff. $r(\text{B}-\text{H}_b)$	1.3	-0.6	1.5	0.6	0.6(10)
$p_9$	$r[\text{B}(1)-\text{H}(1)] - \text{av. } r[\text{B}(4)-\text{H}_i]$	-0.1	-0.4	-0.6	-0.7	-0.7(3)
$p_{10}$	diff. $r(\text{B}-\text{H}_i)$ ( <i>endo</i> - <i>exo</i> )	0.1	0.3	0.2	0.3	0.3(1)
$p_{11}$	av. $r(\text{Ga}-\text{H}_i)$	155.5	155.4	156.2	153.4	153(3)
$p_{12}$	diff. $r(\text{Ga}-\text{H}_i)$ ( <i>endo</i> - <i>exo</i> )	0.0	0.1	0.1	0.2	0.2(1)
$p_{13}$	$\text{B}(3)-\text{B}(1)-\text{H}(1)$	112.1	112.5	111.1	111.8	111.8(10)
$p_{14}$	$\text{H}(2)_{\text{endo}}-\text{Ga}(2)-\text{H}(2)_{\text{exo}}$	129.5	130.4	129.5	131.4	131.4(20)
$p_{15}$	$\text{H}(4)_{\text{endo}}-\text{B}-\text{H}(4)_{\text{exo}}$	119.6	119.7	117.9	119.0	119.0(10)
$p_{16}$	$\text{GaH}_2$ tilt	-2.9	-3.1	-2.4	-2.5	-2.5(6)
$p_{17}$	$\text{BH}_2$ tilt	2.7	0.1	2.7	0.8	0.8(7)
$p_{19}$	$\text{H}(1,2)$ dip	10.2	10.0	11.5	10.5	10.5(10)
$p_{20}$	$\text{H}(1,4)$ dip	3.3	0.1	3.3	0.3	0.3(2)

(b) Vibrational amplitude restraints		
Parameter	Value <sup>c</sup>	Uncertainty <sup>d</sup>
$u_1[\text{B}(1)-\text{B}(3)]$	6.7	0.7
$u_8[\text{Ga}(2)-\text{H}(1,2)]$	13.7	1.4
$u_{11}[\text{B}(1)-\text{B}(4)]$	8.4	0.8
$u_9[\text{Ga}(2)-\text{H}(2)_{\text{endo}}]/u_{10}[\text{Ga}(2)-\text{H}(2)_{\text{exo}}]$	0.999	0.050
$u_{14}[\text{Ga}(2)-\text{H}(1,4)]/u_{13}[\text{Ga}(2)-\text{H}(1)]$	1.024	0.051

<sup>a</sup> For definition of parameters see the text. <sup>b</sup> For method of electron correlation used for Ga see the text. <sup>c</sup> Taken from scaled 6-31G\*/SCF force field. <sup>d</sup> Uncertainties are 5% of amplitude ratio or 10% for direct amplitude restraints.

restraints given in Table 4(b), a further seven amplitudes were successfully refined. Direct amplitude restraints for  $u_1[\text{B}(1)-\text{B}(3)]$  and  $u_{11}[\text{B}(1)-\text{B}(4)]$  were found to be necessary as the normal practice of restraining ratios resulted in the return of unrealistically short vibrational amplitude values in the least-squares refinement, on account of high correlation effects. With the amplitude restraints in place, all amplitudes corresponding to atom pairs contributing 10% or more of the intensity of the most intense feature on the radial-distribution curve were refined. The fixed amplitudes of vibration, all for atom pairs involving hydrogen and of low intensity on the radial-distribution curve, will have little effect on the values or standard deviations of those which were refined.

**Cage structure.** For the three heavy-atom cage distances,  $r[\text{B}(1)-\text{B}(3)]$ ,  $r[\text{B}(1)-\text{B}(4)]$  and  $r[\text{B}(1)\cdots\text{Ga}(2)]$ , the final refined values were 177.9(13), 184.0(13) and 231.0(2) pm, respectively, as compared with the *ab initio* values (6-311G\*\*/MP2) of 178.4, 184.6 and 229.1 pm. The small standard deviation associated with the  $\text{B}(1)\cdots\text{Ga}(2)$  distance reflects the fact that gallium and boron are the two dominant electron scatterers in the molecule. We note that the  $\text{B}(1)\cdots\text{Ga}(2)$  distance, at 231.0(2) pm, differs from the calculated value by ten standard deviations. This reflects the non-convergence of the *ab initio* data, where the parameter value was significantly affected by both basis set and electron correlation effects (see SUP 57390 Table 3). Clearly the experimental value is in this instance better defined than the calculated one. Finally, the butterfly angle ( $p_{18}$ ) refined to  $117.1(7)^\circ$ , compared with its *ab initio* value of  $116.7^\circ$ .

**Bridge region.** The four bridging distances,  $r[\text{B}(1)-\text{H}(1,4)]$ ,  $r[\text{B}(4)-\text{H}(1,4)]$ ,  $r[\text{B}(1)-\text{H}(1,2)]$  and  $r[\text{Ga}(2)-\text{H}(1,2)]$ , refined to 123.7(11), 142.2(18), 123.0(11) and 181(4) pm, respectively. These agree to within one or two standard deviations with their 6-311G\*\*/MP2 calculated *ab initio* values. The distance  $r[\text{Ga}(2)-\text{H}(1,2)]$  is poorly defined by the GED data as a result of its close proximity to the shorter B-B distances; values for  $p_4$  were found to drift between 180 and 199 pm with no

appreciable change in the  $R_G$  factor or in the other refining geometrical parameters. Moreover, the *ab initio* calculations showed a significant variation in this bond length with improvements in basis set and level of theory [see Table 4(a)]. Such a variation was reflected in the uncertainty associated with the flexible restraint, a value of 183(6) pm being adopted. This restraint, although extremely flexible, made it possible to locate the  $r[\text{Ga}(2)-\text{H}(1,2)]$  distance on the radial-distribution curve with greater confidence than was possible on the basis of GED data alone. Overall, however this parameter remains relatively poorly defined.

**Terminal region.** The five terminal B-H and Ga-H distances refined to values slightly shorter than values predicted *ab initio*, with the three B-H distances  $r[\text{B}(1)-\text{H}(1)]$ ,  $r[\text{B}(4)-\text{H}(4)_{\text{endo}}]$ ,  $r[\text{B}(4)-\text{H}(4)_{\text{exo}}]$  agreeing with the *ab initio* predictions to within three standard deviations. The most notable difference between theory and experiment lies with the two Ga-H<sub>t</sub> distances, which were found experimentally to be about 4 pm shorter [149.4(14) and 149.2(14) pm], than the theoretical values (153.5 and 153.3 pm). The new values are, however, some 5 pm longer than those found in the original refinement,<sup>5</sup> and bring results in much closer agreement with those obtained experimentally for other gallium hydrides.<sup>5</sup> The five angles required to describe the terminal B/Ga-H region,  $\text{B}(3)-\text{B}(1)-\text{H}(1)$ ,  $\text{H}(4)_{\text{endo}}-\text{B}(4)-\text{H}(4)_{\text{exo}}$ ,  $\text{H}(2)_{\text{endo}}-\text{Ga}(2)-\text{H}(2)_{\text{exo}}$ ,  $\text{BH}_2$  tilt, and  $\text{GaH}_2$  tilt, all refined to within one standard deviation of the *ab initio* values. Such agreement is expected with the SARACEN method, as the experimental data provide almost no information about these parameters.

The final  $R_G$  factor for the refinement was 0.114, the high value reflecting the noise in the data associated with the fogging of the photographic plates by the  $\text{H}_2\text{GaB}_3\text{H}_8$  vapour. The new structural refinement reported here is a considerable improvement on that previously published.<sup>5</sup> To summarise: firstly a more flexible GED model has been used, comprising an additional six parameters compared to the original model system. Secondly, better approximations to vibrational amplitude values have been obtained from a scaled harmonic *ab initio*

**Table 5** Selected bond distances ( $r_s/\text{pm}$ ) and amplitudes of vibration ( $u/\text{pm}$ ) obtained in the SARACEN study of  $\text{H}_2\text{GaB}_3\text{H}_8$ <sup>a</sup>

<i>i</i>	Atom pair	Distance	Amplitude <sup>b</sup>
1	B(1)–B(3)	180.0(13)	6.7(3)
2	B(1)–H(1)	118.2(8)	8.2 fixed
3	B(1)–H(1,4)	125.2(11)	9.2 fixed
4	B(1)–H(1,2)	124.3(11)	9.1 fixed
5	B(4)–H(1,4)	143.3(18)	11.8 fixed
6	B(4)–H(4) <sub>endo</sub>	119.0(8)	8.3 fixed
7	B(4)–H(4) <sub>exo</sub>	119.0(8)	8.3 fixed
8	Ga(2)–H(1,2)	181(4)	14.7(12)
9	Ga(2)–H(2) <sub>endo</sub>	150.7(14)	14.0(19)
10	Ga(2)–H(2) <sub>exo</sub>	150.5(14)	14.0(19)
11	B(1)–B(4)	184.1(13)	8.4(4)
12	B(1)⋯Ga(2)	231.0(2)	6.3(5)
13	Ga(2)⋯H(1)	314.1(9)	15(2)
14	Ga(2)⋯H(1,4)	314.3(11)	15(2)
15	B(4)⋯Ga(2)	320.2(7)	7.0(10)

<sup>a</sup> Estimated standard deviations, derived from the least-squares refinement, are given in parentheses. <sup>b</sup> Amplitudes which could not be refined are fixed at values derived from the 6-31G\*/SCF scaled force field.

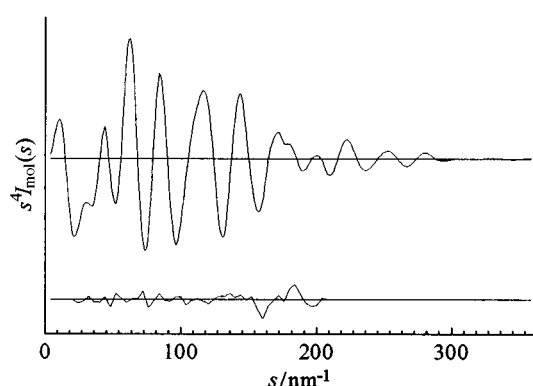


**Fig. 3** Observed and final difference combined molecular scattering curves for  $\text{H}_2\text{GaB}_3\text{H}_8$ . Theoretical data were used in the  $s$  ranges for which no experimental data are available

force field (the previous refinement used rather crude approximations to vibrational amplitudes based on those known from similar compounds). Thirdly, additional structural information has been included from *ab initio* calculations to give a final geometry that is a more complete representation of the true structure of the molecule. Finally (and most importantly) all geometric parameters and all significant vibrational amplitudes are refining. This new structure is free from all constraints and represents the best that can be obtained currently from the available data, both experimental and theoretical; all standard deviations are realistic estimates of the errors and are free from any systematic errors inherent in the limitations of the model.

A selection of bond distances and vibrational amplitude values for the final structure is given in Table 5, the Cartesian coordinates and least-squares correlation matrix are offered in SUP 57390. The final radial-distribution curve and the final combined molecular scattering curve are shown in Figs. 2 and 3, respectively.

### (c) Structural trends within the series $\text{H}_2\text{MB}_3\text{H}_8$ calculated *ab initio*: the effects of changing M

The main structural changes calculated *ab initio* at the 6-311G\*\*/MP2 level for the series of tetraborane(10) derivatives are presented in Table 3. These can be summarised as follows.

**Changes in M–B/H distances.** The increasing values of  $r[\text{B}(1)\cdots\text{M}(2)]$  and  $r[\text{M}(2)\text{–H}(1,2)]$  on moving from B to In can be attributed mainly to the increase in atomic (or ionic)

radius of the atom M (given in Table 3). Significant changes in these parameters occur on replacing boron with aluminium and gallium with indium, but only very small changes are observed on substituting aluminium with gallium. A secondary factor resulting in these structural changes could be the Mulliken charge assignment calculated *ab initio* for atom M (also given in Table 3). As  $\text{M} = \text{B} \longrightarrow \text{In}$  the formal charge calculated for M tends towards +1, *i.e.* the system can be thought of as approaching  $[\text{H}_2\text{M}]^+[\text{B}_3\text{H}_8]^-$ . Owing to this dissociation the distances  $\text{M}(2)\text{–H}(1,2)$  and  $\text{B}(1)\cdots\text{M}(2)$  will increase by an amount greater than the radius of atom M.

**Angles correlated with atom M.** The widening of the angle  $\text{H}(2)_{\text{endo}}\text{–M}(2)\text{–H}(2)_{\text{exo}}$  largely follows the increase in size and decrease in charge calculated on the wing atom M. Atom M is calculated to be more ionic as substitution proceeds down Group 13. The  $\text{H}_2\text{M}$  wing group will therefore tend towards a linear structure and hence the angle will be observed to widen. The bridging angle  $\text{B}(1)\text{–H}(1,2)\text{–M}(2)$  was found to widen in concordance with the increasing distance  $r[\text{B}(1)\cdots\text{M}(2)]$ .

**Changes in  $\text{B}_3\text{H}_8$  fragment.** The distance  $\text{B}(1)\text{–B}(3)$  was found to be affected by the size of atom M, lengthening significantly on replacing boron with aluminium and slightly on replacing gallium with indium, but showing only a very small change on replacing aluminium with gallium, as expected. Similarly, a small narrowing of the  $\text{B}(3)\text{–B}(1)\text{–H}(1)$  angle was observed on moving from boron to indium, but this effect can probably be attributed to a correlation effect with  $r[\text{B}(1)\text{–B}(3)]$ . The distance  $\text{B}(1)\text{–B}(4)$  shortened slightly across the series: from the *ab initio* Mulliken charge assignment this can be attributed to a greater charge disparity between B(1) and B(4) as  $\text{M} = \text{B} \longrightarrow \text{In}$ , and so a simple electrostatic force will cause  $r[\text{B}(1)\text{–B}(4)]$  to shorten over the derivative series.

The  $\text{H}(1,2)$  and  $\text{H}(1,4)$  dip angles reveal that the position of the bridging hydrogen atoms above the BBB/M plane is significantly affected by the identity of atom M. From Table 3 it can be seen that the B–H–M bridging hydrogen atoms are elevated more above the  $\text{B}(1)\text{–M}(2)\text{–B}(3)$  plane [ $\text{H}(1,2)$  dip] than are the B–H–B hydrogen atoms above the  $\text{B}(1)\text{–B}(4)\text{–B}(3)$  plane [ $\text{H}(1,4)$  dip]. This observation can be attributed to the tilting of the two wing units,|| with  $\text{H}_2\text{M}(2)$  tilting on average  $3^\circ$  out of the cage and  $\text{H}_2\text{B}(4)$   $1.5^\circ$  ( $\text{M} = \text{Al} \longrightarrow \text{In}$ ) into the cage. It is reasonable to assume a correlation between the bridging H atoms and the terminal units, and hence the wing tilting should result in  $\text{H}(1,2)$  [and  $\text{H}(2,3)$ ] rising above the  $\text{B}(1)\text{–M}(2)\text{–B}(3)$  plane while  $\text{H}(1,4)$  [and  $\text{H}(3,4)$ ] will flatten into the  $\text{B}(1)\text{–B}(4)\text{–B}(3)$  plane. The variation observed in  $\text{H}(1,2)$  dip as  $\text{M} = \text{B} \longrightarrow \text{In}$  can then be attributed to the increase in size of atom M. Put simply, as M becomes larger the bridging H will seek more space by rising further out of the  $\text{B}(1)\text{–M}(2)\text{–B}(3)$  plane. Note: the value of  $0.3^\circ$  for the  $\text{H}(1,4)$  dip angle in  $\text{H}_2\text{GaB}_3\text{H}_8$  may appear anomalous when compared with the rest of the series but a study of the values returned by the range of *ab initio* calculations performed [see Table 4(a) or SUP 57390 Table 3] indicates that this parameter is not well defined, varying from  $0.1$  to  $3.7^\circ$  depending largely on the quality of basis set used. The true value may well lie in closer agreement with the results obtained for the other members of the series. The final change observed in the  $\text{B}_3\text{H}_8$  fragment relates to the butterfly angle which opened significantly only upon the introduction of indium, thus relieving steric strain between atoms B(4) and In(2).

**Distances and angles unchanged by atom M.** The remaining distances and angles in the  $\text{B}_3\text{H}_8$  fragment  $\{i.e. r[\text{B}(1)\text{–H}(1,4)], r[\text{B}(4)\text{–H}(1,4)], r[\text{B}(1)\text{–H}(1,2)] \text{ and } \text{H}(4)_{\text{endo}}\text{–B}(4)\text{–H}(4)_{\text{exo}}\}$  were effectively independent of the nature atom M.

|| Wing tilts as described in GED model.

## Acknowledgements

We thank the EPSRC for the financial support of the Edinburgh Electron Diffraction Service (grant GR/K44411) and the Edinburgh *ab initio* facilities (grant GR/K04194). We also thank Dr. Lise Hedberg (Oregon State University) for providing us with a copy of the ASYM40 program. Finally, we thank the University of Edinburgh for funding a research studentship for C. A. Morrison.

## References

- 1 S. Cradock, P. B. Liescheski, D. W. H. Rankin and H. E. Robertson, *J. Am. Chem. Soc.*, 1988, **110**, 2758.
- 2 A. J. Blake, P. T. Brain, H. McNab, J. Miller, C. A. Morrison, S. Parsons, D. W. H. Rankin, H. E. Robertson and B. A. Smart, *J. Phys. Chem.*, 1996, **100**, 12 280.
- 3 P. T. Brain, C. A. Morrison, S. Parsons and D. W. H. Rankin, *J. Chem. Soc., Dalton Trans.*, 1996, 4589.
- 4 L. S. Bartell, D. J. Romenesko and T. C. Wong, in *Molecular Structure by Diffraction Methods*, Specialist Periodical Report, The Chemical Society, 1975, vol. 3, p. 72.
- 5 C. R. Pulham, A. J. Downs, D. W. H. Rankin and H. E. Robertson, *J. Chem. Soc., Dalton Trans.*, 1992, 1509.
- 6 C. A. Morrison, B. A. Smart, P. T. Brain, D. W. H. Rankin and A. J. Downs, following paper.
- 7 M. J. Frisch, G. W. Trucks, H. B. Schlegel, P. M. W. Gill, B. G. Johnson, M. A. Robb, J. R. Cheeseman, T. Keith, G. A. Petersson, J. A. Montgomery, K. Raghavachari, M. A. Al-Laham, V. G. Zakrzewski, J. V. Ortiz, J. B. Foresman, J. Cioslowski, B. B. Stefanov, A. Nanayakkara, M. Challacombe, C. Y. Peng, P. Y. Ayala, W. Chen, M. W. Wong, J. L. Andres, E. S. Replogle, R. Gomperts, R. L. Martin, D. J. Fox, J. S. Binkley, D. J. Defrees, J. Baker, J. P. Stewart, M. Head-Gordon, C. Gonzalez and J. A. Pople, GAUSSIAN 94, Revision C.2, Gaussian Inc., Pittsburgh, PA, 1995.
- 8 W. J. Hehre, R. Ditchfield and J. A. Pople, *J. Chem. Phys.*, 1973, **56**, 2257.
- 9 P. C. Hariharan and J. A. Pople, *Theor. Chim. Acta*, 1973, **28**, 213.
- 10 M. S. Gordon, *Chem. Phys. Lett.*, 1980, **76**, 163.
- 11 A. D. McLean and G. S. Chandler, *J. Chem. Phys.*, 1980, **72**, 5639.
- 12 R. Krishnan, J. S. Binkley, R. Seeger and J. A. Pople, *J. Chem. Phys.*, 1980, **72**, 650.
- 13 S. Huzinaga and M. Klobukowski, *J. Mol. Struct.*, 1988, **167**, 1.
- 14 L. Hedberg and I. M. Mills, ASYM40, version 3.0, update of program ASYM20, *J. Mol. Spectrosc.*, 1993, **160**, 117.
- 15 A. S. F. Boyd, G. S. Laurensen and D. W. H. Rankin, *J. Mol. Struct.*, 1981, **71**, 217.
- 16 A. W. Ross, M. Fink and R. Hilderbrandt, *International Tables for Crystallography*, ed. A. J. C. Wilson, Kluwer, Dordrecht, Boston and London, 1992, vol. C, p. 245.
- 17 M. Bühl and P. v. R. Schleyer, *J. Am. Chem. Soc.*, 1992, **114**, 477.
- 18 T. H. Dunning and P. J. Hay, *Modern Theoretical Chemistry*, Plenum, New York, 1996, ch. 1, pp. 1–28.
- 19 M. L. McKee, *Chem. Phys. Lett.*, 1991, **183**, 510.
- 20 B. J. Duke and H. F. Schaefer III, *J. Chem. Soc., Chem. Commun.*, 1991, 123.
- 21 D. D. Ebbing, *General Chemistry*, ed. M. S. Wrighton, Houghton Mifflin, Boston, 1987, ch. 7.
- 22 C. J. Dain, A. J. Downs, G. S. Laurensen and D. W. H. Rankin, *J. Chem. Soc., Dalton Trans.*, 1981, 472.
- 23 C. J. Dain, A. J. Downs and D. W. H. Rankin, *J. Chem. Soc., Dalton Trans.*, 1981, 2465.
- 24 M. J. Goode, A. J. Downs, C. R. Pulham, D. W. H. Rankin and H. E. Robertson, *J. Chem. Soc., Chem. Commun.*, 1988, 768.

Received 24th February 1998; Paper 8/01553H